Journal of Analytical and Applied Pyrolysis 125 (2017) 32–39

Contents lists available at ScienceDirect

Journal of Analytical and Applied Pyrolysis

journal homepage: www.elsevier.com/locate/jaap

Development of Ni- and Fe- based catalysts with different metal particle sizes for the production of carbon nanotubes and hydrogen from thermo-chemical conversion of waste plastics

Xiaotong Liu[a], Yeshui Zhang[b], Mohamad A. Nahil[b], Paul T. Williams[b,*], Chunfei Wu[a,*]

[a] School of Engineering, University of Hull, Hull, HU6 7RX, UK
[b] School of Chemical & Process Engineering, University of Leeds,Leeds, LS2 9JT, UK

ARTICLE INFO

Keywords:
Hydrogen
Carbon nanotubes
Iron
Nickel
Catalyst

ABSTRACT

Co-production of valuable hydrogen and carbon nanotubes (CNTs) has obtained growing interest for the management of waste plastics through thermo-chemical conversion technology. Catalyst development is one of the key factors for this process to improve hydrogen production and the quality of CNTs. In this work, Ni/SiO_2 and Fe/SiO_2 catalysts with different metal particle sizes were investigated in relation to their performance on the production of hydrogen and CNTs from catalytic gasification of waste polypropylene, using a two-stage fixed-bed reaction system. The influences of the type of metals and the crystal size of metal particles on product yields and the production of CNTs in terms of morphology have been studied using a range of techniques; gas chromatography (GC); X-ray diffraction (XRD); temperature programme oxidation (TPO); scanning electron microscopy (SEM); transmission electron microscopy (TEM) etc. The results show that the Fe-based catalysts, in particular with large particle size (~80 nm), produced the highest yield of hydrogen (~25.60 mmol H_2 g^{-1} plastic) and the highest yield of carbons (29 wt.%), as well as the largest fraction of graphite carbons (as obtained from TPO analysis of the reacted catalyst). Both Fe- and Ni-based catalysts with larger metal particles produced higher yield of hydrogen compared with the catalysts with smaller metal particles, respectively. Furthermore, the CNTs formed using the Ni/SiO_2-S catalyst (with the smallest metal particles around 8 nm) produced large amount of amorphous carbons, which are undesirable for the process of CNTs production.

1. Introduction

Plastics are one of the most widely-used and multi-purpose materials. Due to increasing demand, global plastics production has continuously grown to 322 million tonnes in 2015, indicating a nearly 60% increase compared to the level in 1990 [1]. Recycling, energy recovery and landfill are the three main treatment options for plastics waste. At the moment, landfill is still largely used (~31 wt.%) in many EU countries, causing significant environmental problems and wasting the energy stored inside the plastics [2]. Therefore, converting waste plastics into valuable products e.g. hydrogen enriched syngas is promising as an alternative method for the management of waste plastics.

Hydrogen is a clean and efficient energy carrier and considered as an alternative fuel for the future. It is known that the use of catalysts is key to maximize the production of hydrogen during the thermo-chemical conversion process [3–6]. Many catalysts have been studied to improve hydrogen production from gasification of waste plastic. For example, Nanioka et al. [7] used Ru based catalysts to enhance hydrogen production from steam gasification of polystyrene using a fixed-bed reactor. A two-stage continuous reactor was used to optimize process conditions including reaction temperature and weight space velocity for gasification of polypropylene using Ru based catalysts [8]. In addition, Elordi et al. [9] used HZSM-zeolite with different ratios of SiO_2/Al_2O_3 as catalyst to investigate coke formation during hydrogen production from gasification of mixed plastics waste. However, it is known that noble-based catalysts are expensive for gasification of waste plastics. Cost effective Fe, Mo, Co and Ni supported on SiO_2, Al_2O_3, and MgO are effective catalysts for hydrogen production through hydrocarbon reforming reactions [10,11]. For example, high H_2 (29.1 wt%) yield was produced from polystyrene gasification by using Ni-based catalysts [12]. However, the formation of coke on the surface of catalysts and the problem of catalyst sintering are the two main challenges for the development of catalysts for the process. Ni catalysts supported on different metal oxides including Al_2O_3, ZrO_2, TiO_2, MgO and Ce_mO_2 and Cu/Mg/Al have been investigated with the aim to

* Corresponding authors.
E-mail addresses: p.t.williams@leeds.ac.uk (P.T. Williams), c.wu@hull.ac.uk (C. Wu).

http://dx.doi.org/10.1016/j.jaap.2017.05.001
Received 23 January 2017; Received in revised form 29 March 2017; Accepted 2 May 2017
Available online 03 May 2017

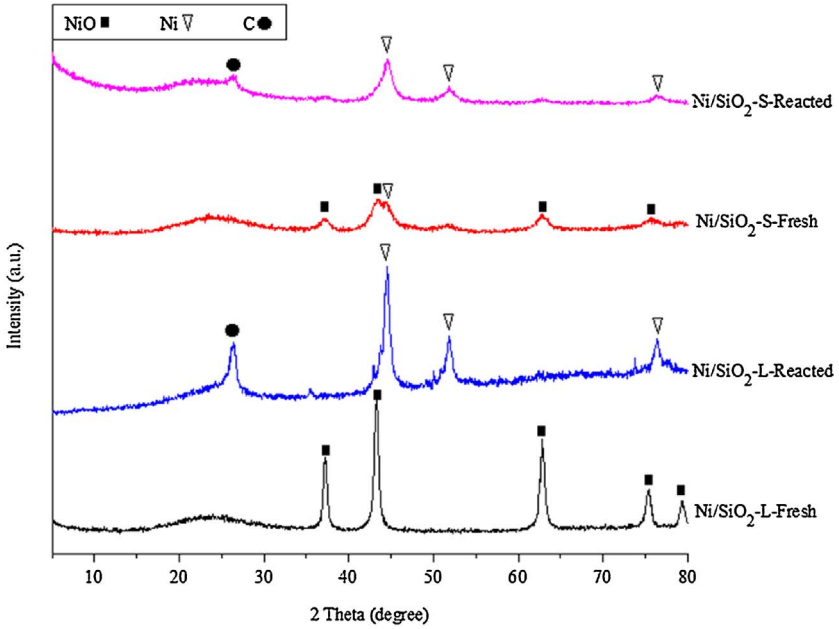

Fig. 1. XRD results for Ni-based catalysts before and after reaction.

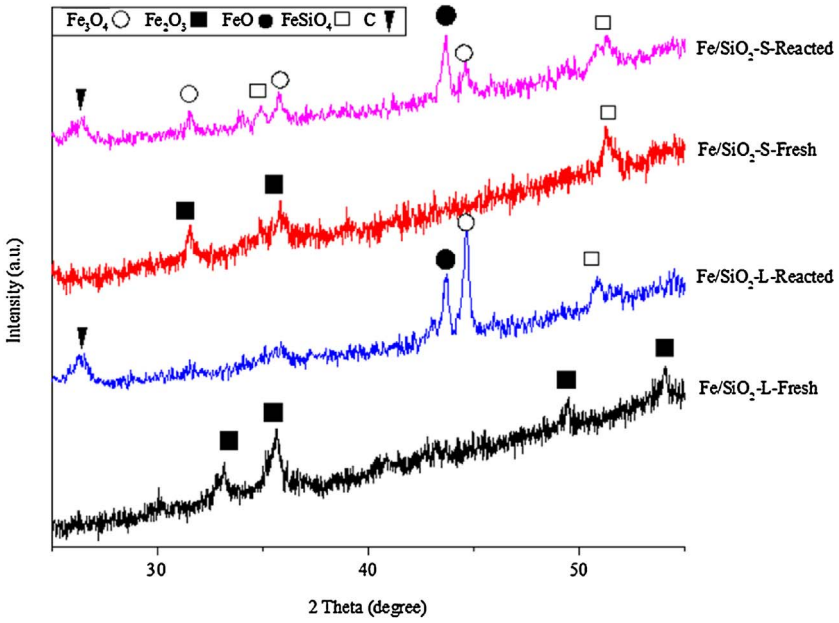

Fig. 2. XRD results for Fe-based catalysts before and after reactions.

reduce the formation of coke on the surface of the reacted catalyst [13–15].

In addition, several co-precipitated nickel-based catalysts have been investigated for hydrogen production from pyrolysis-gasification of polypropylene. Ni-Al (molar ratio 1:2) and Ni-Mg-Al (molar ratio 1:1:2) catalysts were found to show the most enhanced catalytic effectiveness in terms of H_2 production and the prevention of coke formation [16–18]. However, the formation of carbon on the reacted catalyst is largely un-avoidable. Producing carbon nanotubes (CNTs) together with hydrogen from waste plastics seems to be a promising development to maximize the economic feasibility of the process. CNTs are valuable materials having specific mechanical and electronic properties and has broad applications in the fields of energy and environmental protection [19,20].

Ni-Al catalysts doped with Ca and Zn have been investigated for the production of both hydrogen and CNTs from waste plastics [21]. Compared to Ni/Ca-Al catalyst, Ni/Zn-Al catalyst have been reported to produce higher yields of H_2, but with less production of CNTs, due to the promotion of catalytic interactions between steam and carbon containing compounds [16,21]. Zhao et al. [22] produced CNTs with uniform diameter and high quality using Ni-loaded catalysts from the reforming of ethanol. Ago et al. [10] synthesised CNTs with Ni and Fe-based catalysts supported by MgO using CH_4 as feedstock, and found that it was difficult to produce CNTs from Ni-based catalysts; they suggested that Ni-based catalysts had low metal diffusivity and carbon solubility.

The formation of CNTs depends on experimental parameters such as, catalyst particle size [23] and it has been suggested that the size of metal particles used in chemical vapor deposition could define the diameters of the CNTs growth [24]. For example, Baker et al. [25] and Kim et al. [26] reported that the growth of carbon nanotubes was governed by associated catalytic particles. However, there are few

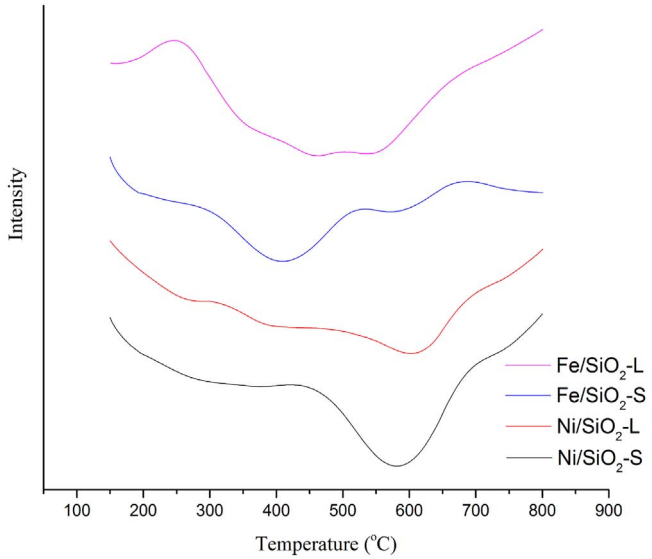

Fig. 3. TPR results for fresh catalysts.

studies concerned with using Ni and Fe based catalysts for producing CNTs using waste plastics as feedstock.

This work aims to investigate the influences of the types of metal (Fe and Ni) and the particle size of the metals on the catalyst in relation to the production of CNTs and hydrogen from thermo-chemical conversion of waste plastics.

2. Materials and methods

2.1. Materials

The raw material plastic used in this research was waste polypropylene (PP) pellets with 2 mm diameter obtained from regain polymers Ltd. Ni/SiO_2 and Fe/SiO_2 catalysts were synthesised by a sol-gel method. During the preparation of the catalysts, the required amount of Ni $(NO_3)_2{\cdot}6H_2O$ or $Fe(NO_3)_3{\cdot}9H_2O$ and tetrathoxysilane (TEOS) were dissolved in ethanol. The mixture was stirred for one hour at a temperature of 60 °C, and dried at 100 °C overnight. The obtained catalyst precursors were calcined in N_2 and air, respectively, at 750 °C with 10 °C min^{-1} heating rate for 3 h. All the catalysts used in this study were reduced under H_2 for 1 h prior to the experimental tests. Finally, the prepared catalysts were ground and sieved to particle sizes below 50 μm. Catalysts calcined in N_2 were designated as 'S' as an indication of the catalyst with small metal particles, and calcined in air were designated as 'L' indicating large metal particles.

2.2. Gasification of plastics waste using Ni and Fe-based catalysts

A two-stage catalytic-gasification reaction system consisting of a plastic pyrolysis stage and a catalytic gasification stage was used in this study. In each experiment, when the catalytic temperature was stabilized at desired temperature, about 1 g waste polypropylene was pyrolysed inside the first stage which was heated from room temperature to 600 °C. The vapours produced from pyrolysis passed the second reaction stage where 0.4 g catalyst was located. The second catalytic stage temperature was 800 °C. N_2 was used as carrier gas with 80 ml min^{-1} flow rate. The total reaction time was 50 min. Two condensers were used to trap the condensable products including water and dry ice condensation. The non-condensed gases were collected by a 25 L Tedlar™ gas sample bag for further analysis.

The collected gas samples were analyzed off-line by two groups of gas chromatographs (GC). Hydrocarbons (C_1–C_4) were analyzed using a Varian 3380 gas chromatograph with a flame ionization detector, a 80–100 mesh HayeSep column and nitrogen as carrier gas. The permanent gases including hydrogen, oxygen, carbon monoxide and nitrogen, were analyzed by a second Varian 3380 GC with two separate columns, using a 60–80 mesh molecular sieve column with argon carrier gas, whilst carbon dioxide was analyzed with a HayeSep 80–100 mesh column.

2.3. Characterization of fresh and reacted catalysts

The BET (Brunauer, Emmett and Teller) surface area of each catalyst was determined by nitrogen adsorption experiments using a Quantachrome Corporation (FL, US) Autosorb 1-C Instrument. A high resolution scanning electron microscope (SEM) and a transmission electron microscope (TEM) were used to study the surface morphology of the Ni- and Fe-based catalysts, and the diameters of metal particles had also been analyzed by TEM. Fresh and reacted catalysts were characterized by X-ray diffraction (XRD), and the data was analyzed with Stoe IPDS2 software. Temperature programmed oxidation (TPO) of the reacted catalysts was analyzed to obtain information of coke formation on the surface of the reacted catalyst and the reducibility of the fresh catalysts was determined using temperature programmed reduction (TPR) with a thermogravimetric analyser (TGA) STA-780 series. During the TPO analysis, around 10 mg of the reacted catalyst was heated in an atmosphere of air at 10 °C min^{-1} to a final temperature of 800 °C. For the TPR analysis, the fresh catalyst was heated at 40 °C min^{-1}–150 °C and held for 10 min, then heated at 10 °C min^{-1}–800 °C in an atmosphere consisting of a gas mixture 5 vol. %H_2 and 95 vol. %N_2 with 50 ml min^{-1} flow rate.

3. Results and discussion

3.1. Characterizations of the fresh catalysts

XRD results of the Ni- and Fe-based catalysts are shown in Figs. 1 and 2, respectively. From Fig. 1, the presence of NiO and Ni are shown in both Ni-based catalysts. The fresh Ni/SiO_2-L catalysts showed four main sharp NiO peaks at 37°, 43°, 64° and 71° [27,28]. Weak Ni diffraction peaks were observed in the Ni/SiO_2-S catalyst at 44° and 52° [29]. It is indicated that large Ni-based species are present in the Ni/SiO_2-L catalyst, while small Ni-based species were found in the Ni/SiO_2-S catalyst. In addition, a diffraction peak at 27° was observed indicating the presence of graphite carbon on the surface of the reacted Ni/SiO_2 catalyst. As shown in Fig. 1, sharp diffraction peaks of Ni were observed for the Ni/SiO_2-L-reacted catalyst, compared with the Ni/SiO_2-S-reacted catalyst, indicating that larger Ni particles were produced in the reacted Ni/SiO_2-L catalyst as expected. Fig. 2 shows the presence of Fe_3O_4 [30] on the fresh and reacted Fe-based catalysts, suggesting that Fe_2O_3 particles contented in the fresh Fe/SiO_2 catalyst were reduced during the thermo-chemical conversion process. Diffraction of graphite carbon was also observed for the reacted Fe/SiO_2 catalysts with small and large metal particles. Furthermore, compared to the Fe/SiO_2-S, sharp diffraction peaks were observed for the Fe/SiO_2-L catalyst, supporting that large metal particles were formed in the Fe/SiO_2-L catalyst.

Results of TPR analysis for the fresh Ni- and Fe-based catalysts were shown in Fig. 3. The first reduction peak for the Fe-based catalysts appeared at temperature between 380 and 450 °C, ascribed to the reduction of Fe_2O_3 and FeO. The second reduction peak for the Fe-based catalysts was shown at temperature around 600 °C, which was attributed to the further reductions of Fe^{2+} [30]. High reduction temperature (around 590 °C) was observed for the Ni-based catalyst, which might be due to that Ni particles were much smaller compared with Fe-based particles. It was reported that higher temperature was required to reduce catalysts with small metal oxide particles [31].

As measured from TEM micrographs (Fig. 4A–D), the diameter of metal particles of the fresh catalyst (Fig. 4a–d) was around 85 nm for

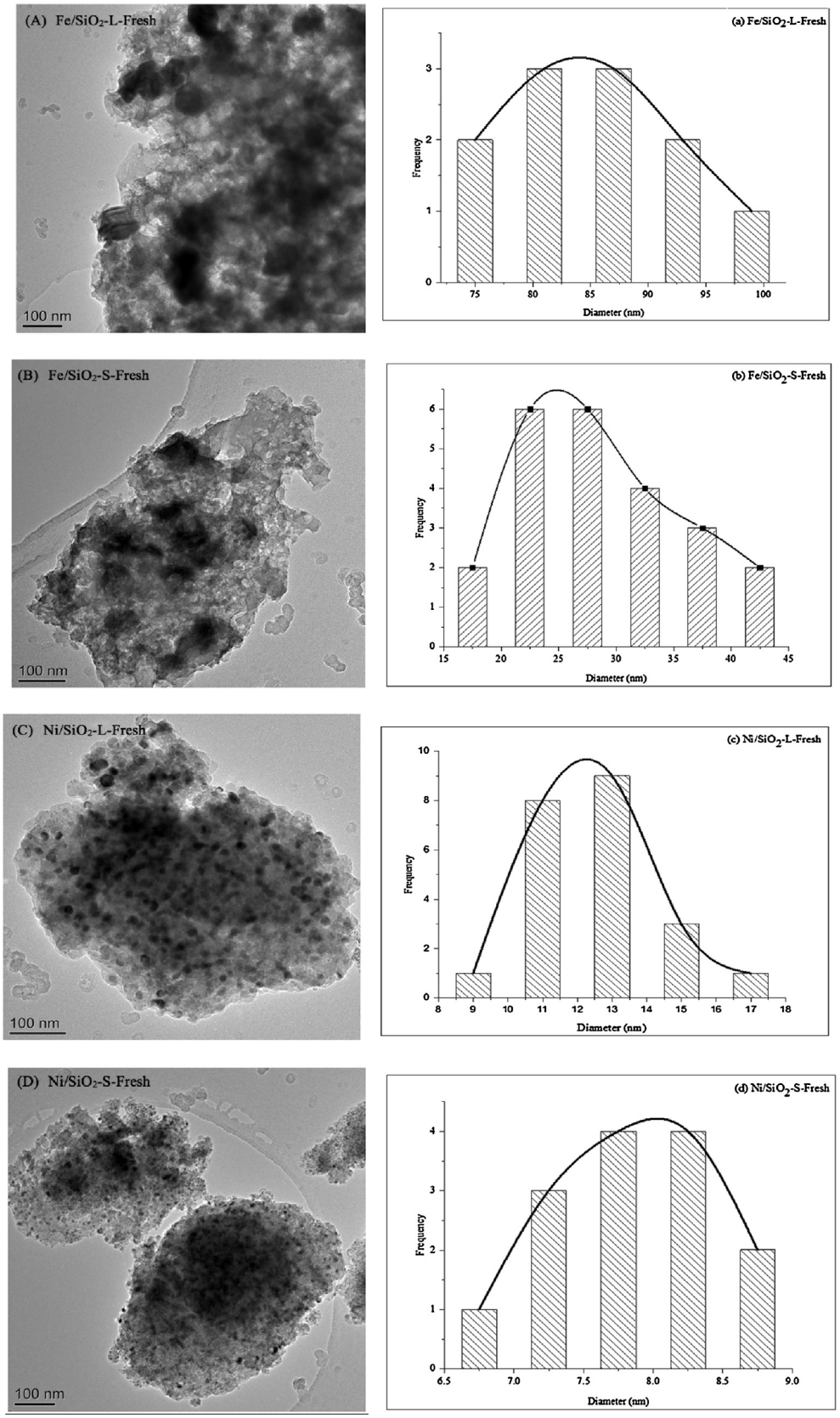

Fig. 4. TEM results for fresh catalysts (A) Ni/SiO_2-L-fresh (B) Ni/SiO_2-S-fresh (C) Fe/SiO_2-L-fresh (D) Fe/SiO_2-S-fresh, and analysis for metal particles sizes (a) Ni/SiO_2-L-fresh (b) Ni/SiO_2-S-fresh (c) Fe/SiO_2-L-fresh (d) Fe/SiO_2-S-fresh.

the Fe/SiO_2-L, 29 nm for the Fe/SiO_2-S, 13 nm for the Ni/SiO_2-L, and 8 nm for the Ni/SiO_2-S, respectively. Therefore, larger particle sizes were clearly observed on the Ni/SiO_2-L-fresh and the Fe/SiO_2-L-fresh catalysts, compared to the Ni/SiO_2-S-fresh and the Fe/SiO_2-S-fresh catalysts, respectively. The results are consistent with the XRD analysis and TPR analysis (Fig. 3), where much higher temperature was required

Table 1
Production yield and gas composition from catalytic gasification of PP by using Ni- and Fe-based catalysts.

	Fe/SiO_2-S	Fe/SiO_2-L	Ni/SiO_2-S	Ni/SiO_2-L
Gas yield (wt.%)	49.20	63.90	51.20	52.50
Carbon production (wt.%)[a]	26.00	29.00	16.00	16.00
H_2 production (mmol g^{-1} plastics)	15.40	25.60	18.10	22.60
Gas concentrations (vol.%)				
CO	5.32	7.80	3.30	6.32
H_2	41.72	50.30	42.20	47.74
CH_4	39.16	22.70	43.50	38.31
C_2–C_4	13.80	19.20	11.00	7.62

[a] Obtained from the weight difference of the reactor tube before and after experiment.

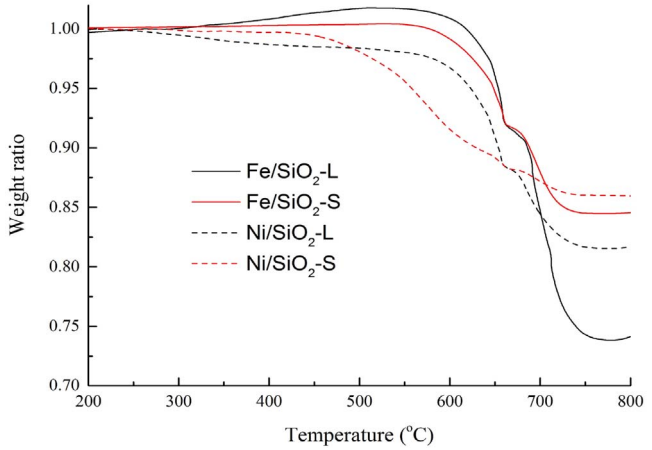

Fig. 5. TPO results for Fe- and Ni-based catalysts after reaction.

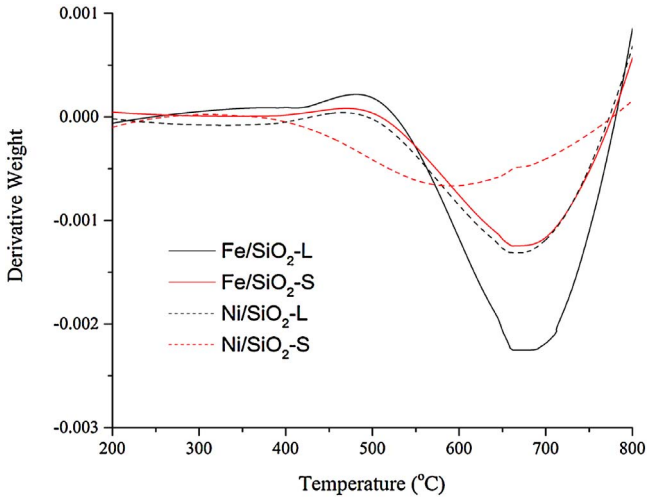

Fig. 6. DTG-TPO results of the reacted Fe- and Ni-based catalysts.

for the reduction of the Ni-based catalysts compared with the Fe-based catalysts. In addition, from the TEM analysis, the Fe-based catalysts show larger particle sizes than the Ni-catalysts.

3.2. Gas yield and composition

Table summarizes the influence of different catalysts on the production of gas and hydrogen, as well as the yield of carbon from the catalytic thermo-chemical conversion of waste plastic. Regarding the yield of hydrogen production, the following trend was observed: Fe/SiO_2-L > Ni/SiO_2-L > Ni/SiO_2-S > Fe/SiO_2-S (Table 1). It seems that the catalyst with large particle size was more effective for H_2 production in this work, when the same metal based catalyst was used. For example, hydrogen production was increased from 15.40 to 25.60 (mmol g^{-1} plastic), when the catalyst was changed from the Fe/SiO_2-S to the Fe/SiO_2-L catalyst. The hydrogen yield was also increased from 18.10 to 22.60 (mmol g^{-1} plastic), when the catalyst was changed from the Ni/SiO_2-S to the Ni/SiO_2-L catalyst. In addition, hydrogen concentration was around 41 vol.% using catalysts with small metal particles, and was increased to around 50 vol.%, when the catalysts with large metal particles were used for polypropylene gasification. The enhanced hydrogen production with the increase of metal particle size corresponds to the reduction of CH_4 concentration from 39.16 to 22.70 vol.%. Similar trend is also observed for the Ni-based catalyst, as the reduction of Ni particle size resulted in a reduction of CH_4 concentration from 43.50 to 38.31 vol.%. Hydrogen production in this work was similar compared to a previous study (~20 mmol H_2 g^{-1} sample) using Ni-Mg-Al catalyst for thermo-chemical conversion of polyethylene under N_2 atmosphere [32]. However, the hydrogen production was much lower than literature using steam gasification [33], when steam contributed a large fraction of hydrogen source An increase of particle size of Pt from 2.97 to 3.56 nm resulted in an increase of gas yield during catalytic steam reforming of glycerol, when 5% Pt/C-black catalysts were used [34].

However, catalyst with smaller Ni-particles was reported to produce higher yields of gas and hydrogen, when various Ni/MCM-41 catalysts were used for gasification of biomass; it was reported that small metal particles resulted in a better dispersion of active sites [35]. When mesoporous SBA-15 support was used with 5 wt.% metal loading for dry reforming of methane, catalyst with smaller metal particles (~5 nm) was reported to have higher metal dispersion and exhibited excellent catalytic activity for methane conversion and catalytic stability, compared with same metal loading catalysts with larger Ni particles (~9 nm) [36]. Herein, it is suggested that the influence of metal particle size on gas and hydrogen production might be related to the feedstock and the support of catalyst. Compared to the previous report using biomass and MCM-41 as catalyst support, in this work, waste plastic was used with disordered SiO_2 as catalyst support. However, the better performance of the catalysts with larger metal particle sizes in relation to hydrogen production might be also due to the higher pore volume of the catalysts, compared to the catalyst with smaller metal particle sizes. For example, the total pore volumes of the Fe/SiO_2-L-fresh and the Fe/SiO_2-S-fresh catalysts are 0.287 cm^3 g^{-1} and 0.096 cm^3 g^{-1}, respectively. The total pore volumes of the Ni/SiO_2-L-fresh and the Ni/SiO_2-S-fresh catalysts are 0.314 cm^3 g^{-1} and 0.260 cm^3 g^{-1}, respectively. Smaller metal particles might block the pores inside catalyst. Thus, for the Fe/SiO_2-S-fresh catalyst, the diffusion of volatile molecules inside the catalyst was limited, resulting in a lower production of hydrogen.

In this work, the ion-based catalyst with large Ni particles produced the highest production of hydrogen. Nickel-based catalysts have been reported to promote hydrogen yield compared to iron based catalysts during hydrogen production from catalytic steam reforming of ethanol [37]. In addition, nickel catalysts are widely studied for hydrogen production compared to iron, however, in this study, the Fe/SiO_2-L has shown better performance in terms of hydrogen production compared with the nickel catalysts. Iron based catalyst has also been reported to have higher hydrogen production compared to nickel based catalyst, when different metal based catalysts were investigated for hydrogen production from pyrolysis of plastics feedstocks. [38]. Therefore, it is suggested that a large amount of carbon formation could result in a high yield of hydrogen due to hydrocarbon decomposition reactions, as shown in Eq. (1). As shown in Table 1, the Fe/SiO_2-L catalyst produced the highest yield of carbon (29% in relation to the weight of plastic), while the Ni-based catalysts produced a relative low yield of carbon (16 wt.%).

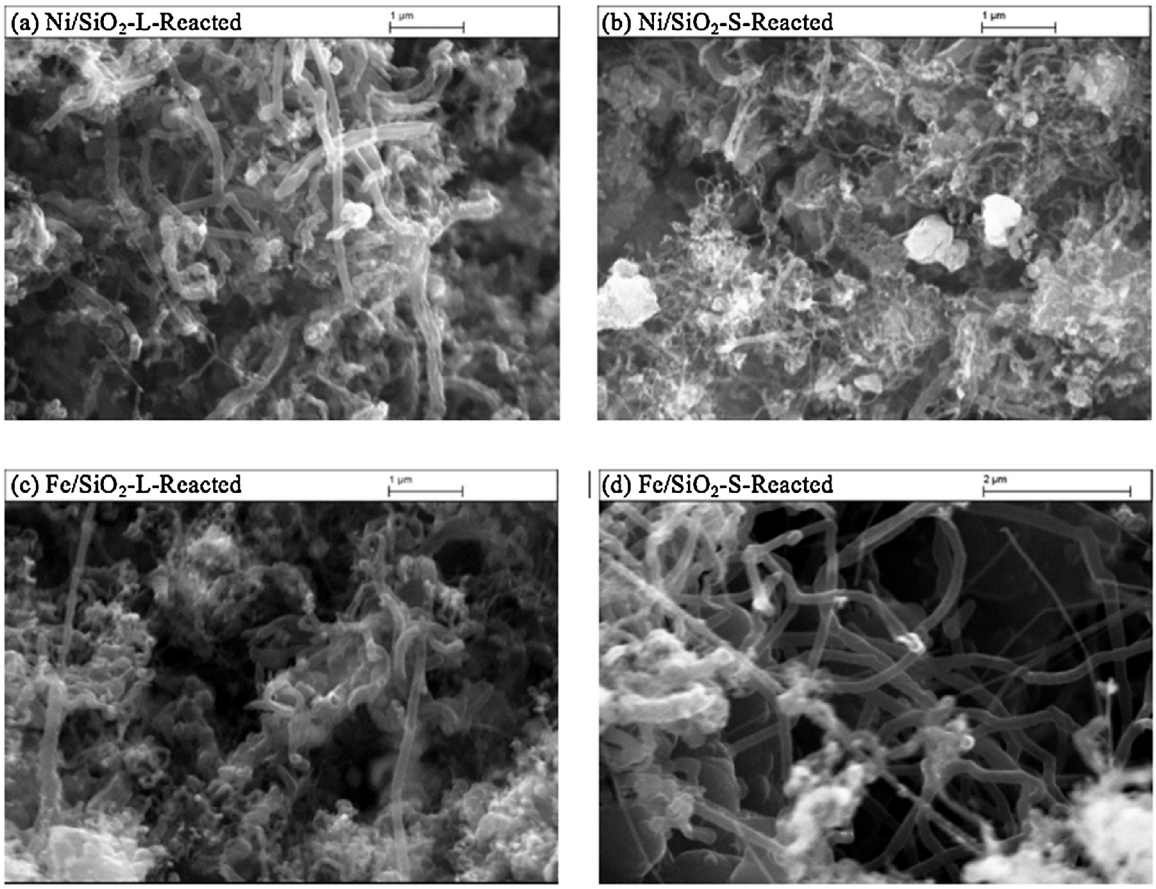

Fig. 7. SEM results for catalysts after reaction.

$$C_nH_m \rightarrow C + H_2 \quad (1)$$

3.3. The production of CNTs

3.3.1. The influence of metal species on CNTs production

The reacted Fe- and Ni-based catalysts were analyzed by TPO experiments (Fig. 5) and DTG curves (Fig. 6). Three stages of carbon oxidation were identified: i) amorphous carbons (~550 °C), ii) filamentous carbons with small diameters (~660 °C) and iii) filamentous carbons with large diameters (~730 °C) [10]. The reacted Ni/SiO_2-S catalyst showed significant weight loss at low temperature (~400 °C) compared to the other catalysts, clearly been seen from DTG curves (Fig. 6), suggesting that high amounts of amorphous carbons were formed using the Ni/SiO_2-S catalyst. SEM analysis (Fig. 7) of the reacted catalysts confirms that the morphology of the CNTs formed on the surface of the Ni/SiO_2-S catalyst was poor compared to the other reacted catalysts.

From Figs. 5 and 6, the oxidation temperature of graphite type carbons (after 600 °C) formed on the reacted Fe/SiO_2-L catalyst was higher compared to other catalysts. This is also consistent with the carbon yield as shown in Table 1, where the Fe/SiO_2-L catalyst resulted in the highest yield of carbon. Fe has been reported to be preferable for the precipitation of graphitic carbons instead of amorphous carbon during the thermo-chemical conversion of polypropylene [29]. In addition, there was slightly weight increase from 400 °C for the Fe/SiO_2-L and Fe/SiO_2-S catalysts (Figs. 5 and 6), that could be resulted from the oxidation of Fe_3O_4 in the TPO process. However, in this work, it is suggested that the oxidation of metallic metal was not significant in the TPO analysis.

Similar results were found by Lee et al. [39] who studied CNTs growth with Ni, Fe and Co catalysts on a silica support using C_2H_2 as feedstock; they reported that Fe-based catalyst produced the highest quality CNTs with homogeneous distributions. It is suggested that the interaction between catalytic metals and support played a key role in the growth of CNTs. A weak interaction between metal and catalyst support was suggested to promote the growth of CNTs, while a strong interaction restricted the availability of metal particles and thus prohibited the production of CNTs [40]. According to the tip-growth mechanism, metal particles are involved in the growth of CNTs. The stronger metal-support interaction that occurs; the less metal particles are available to grow CNTs. In contrast, too weak a metal support interaction might cause the sintering of metal during high temperature reactions. The stronger interaction between Ni particle and SiO_2 support (higher reduction temperature was required for Ni-based catalyst as shown in Fig. 4) might be ascribed to the poor production of CNTs in this work. Previously, we [38] investigated the production of CNTs from gasification of plastic using Fe, Ni, Co and Cu-based catalyst and reported that Fe-based catalyst produced CNTs with better quality in terms of the yield and purity. Carbon solubility was suggested as an important factor governing CNTs production, the driving force for CNTs growth was enhanced with the increase of carbon solubility [41,42]. The large carbon solubility of iron particles might be responsible for the better performance during the formation of CNTs [43,44].

3.3.2. The influence of metal particle size on CNTs production

TEM analysis (Fig. 8) for the reacted catalysts shows that the diameter of CNT is about 98 nm for the Fe/SiO_2-L, 50 nm for the Fe/SiO_2-S, 23 nm for the Ni/SiO_2-L, and 18 nm for the Ni/SiO_2-S, respectively. Compared to the metal particle size of the fresh catalysts (Fig. 4), the same order of metal particle size has been observed with Fe/SiO_2-L (85 nm) > Fe/SiO_2-S (29 nm) > Ni/SiO_2-L (13 nm) > Ni/SiO_2-S (8 nm). Therefore, it is demonstrated that the diameters of

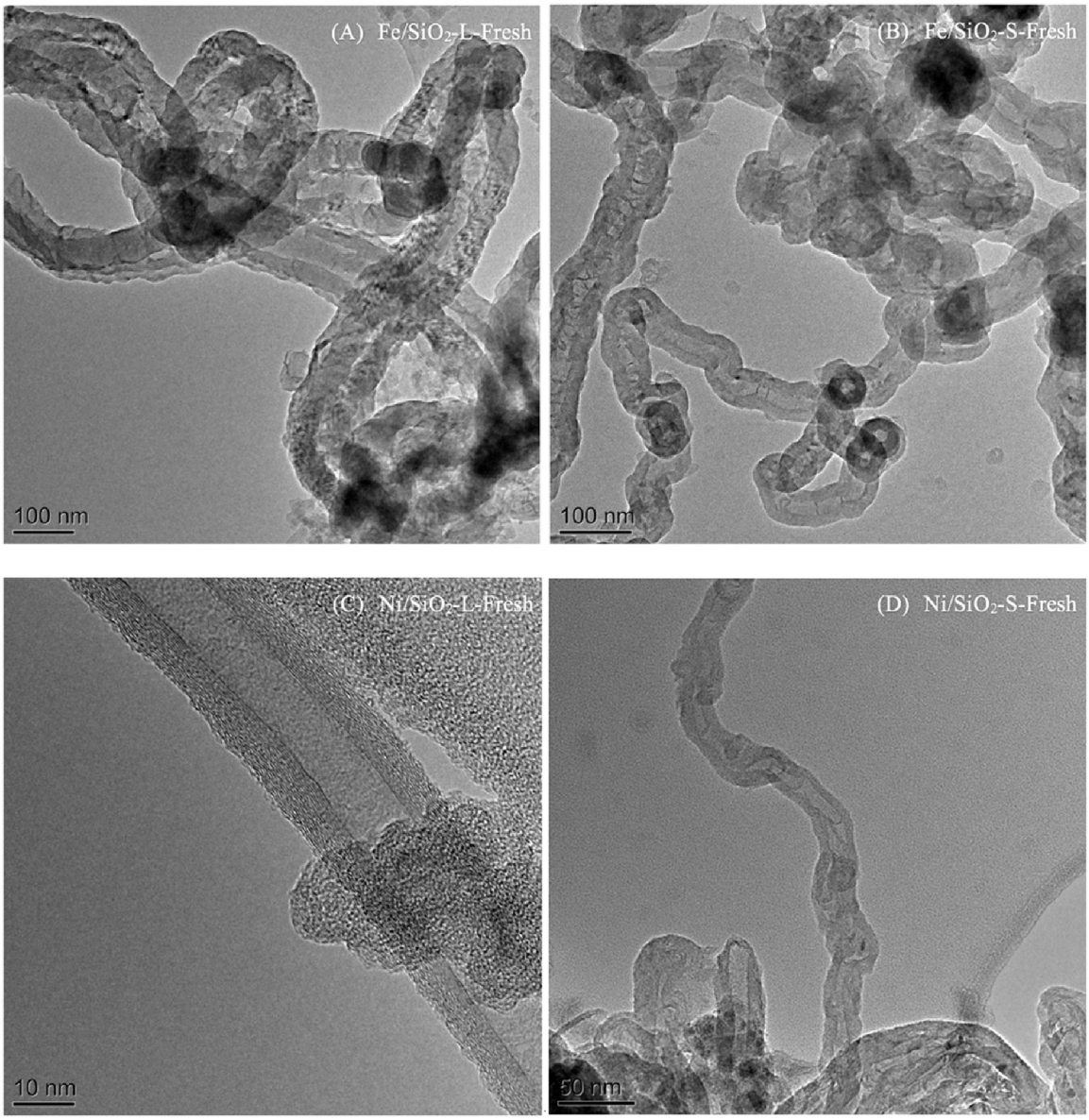

Fig. 8. TEM results for reacted catalysts (a) Fe-L-Reacted (98 nm) (b) Fe-S-Reacted (50 nm) (c) Ni-L-Reacted (23 nm) (d) Ni-S-Reacted (18 nm).

CNTs grown depends on the metal sizes of catalysts.

As shown in Table 1, the yield of carbon was increased from 26.00 to 29.00 wt.%, when the Fe/SiO_2-L catalyst was used, compared to the Fe/SiO_2-S catalyst. In addition, the carbon production was also increased using the Ni-based catalyst, when the size of metal particles was increase from around 8 nm to 13 nm (Fig. 4 and Table 1).

Large metal particle size was reported to generate increased yield of carbon deposition on reacted catalyst during catalytic steam reforming of ethanol [45]. The authors proposed that carbon formation was related to a lower fraction of terrace atoms corresponding to a reducing number of unsaturated metal surface atoms, when catalyst with large metal particles was used during the ethanol steam reforming process. The formation of carbon during catalytic conversion of hydrocarbons was also suggested to require relative large domains of flat terraces of metal particles [46]. Chen et al. [47]. investigated the influence of Ni particle size on the production of carbon fibers through methane decomposition. They concluded that an optimal metal size of Ni (~34 nm) was found to be effective for the growth of carbon nanofibers, because smaller Ni particles resulted in a high saturation and a low diffusion of carbon atoms and thus leading to a low production of carbon nanofibers. Furthermore, they suggested that a slow decomposition of hydrocarbons on the surface of metal particles was observed when large crystal Ni particles were presented due to the low surface area of metal particles. This is consistent with the results showing in this work, where the particle size of NiO of around 23 nm was found to produce higher yield of carbon compared to the Ni/SiO_2-S catalyst having NiO particle sizes around 8 nm.

In addition, Cheung et al. [48] carried out a diameter-controlled synthesis of carbon nanotubes using iron particles with different diameters (3, 9 and 13 nm); CNTs with average diameters of 3, 7 and 12 nm were reported to be produced, respectively. Ding et al. [49] carried out a molecular dynamic study in relation to the influence of catalyst particle size on growth mechanism and structure of carbon nanotubes. They reported that large catalyst particles containing at least 20 atoms generated CNTs with much better tubular structure compared to CNTs nucleated from smaller clusters [49].

4. Conclusions

Carbon nanotubes and hydrogen were successfully produced from thermo-chemical processing of waste polypropylene using Ni/SiO_2 and Fe/SiO_2 catalysts with different particle sizes. The Fe-based catalyst

with the largest metal particles resulted in the highest hydrogen production (25.60 mmol g^{-1} plastic) and the highest yield of carbon (29 wt.%). It is suggested to be due to a high carbon solubility of iron metal particles compared to Ni-based catalysts. The consistency between metal particle size and the diameter of CNTs was observed in this work, as the catalysts with different metal particle sizes generated the CNTs with the corresponding diameters. In addition, a strong interaction between Ni and SiO_2 support is suggested to suppress the growth of CNTs, while many amorphous carbons were produced using the Ni/SiO_2-S catalyst.

Acknowledgement

This project has received funding from the European Union's Horizon 2020 research and innovation programme under the Marie Sklodowska-Curie grant agreement No. 643322 (FLEXI-PYROCAT).

References

[1] Plastics Europe, 2016 plastics Europe, (2016).
[2] Plastics Europe, 2015 Plastics Europe, (2015).
[3] T. Namioka, A. Saito, Y. Inoue, Y. Park, T.J. Min, S.A. Roh, K. Yoshikawa, Appl. Energy 88 (2011) 2019.
[4] J. Liu, Z.W. Jiang, H.O. Tang, T. Tang, Polym. Degrad. Stab. 96 (2011) 1711.
[5] M.Y. He, Z.Q. Hu, B. Xiao, J.F. Li, X.J. Guo, S.Y. Luo, F. Yang, Y. Feng, G.J. Yang, S.M. Liu, Int. J. Hydrogen Energy 34 (2009) 195.
[6] A.M. Brass, J. Chene, Mater. Sci. Eng. A-Struct. 242 (1998) 210.
[7] T. Namioka, A. Saito, Y. Inoue, Y. Park, T.-j. Min, S.-a. Roh, K. Yoshikawa, Appl. Energy 88 (2011) 2019.
[8] Y. Park, T. Namioka, S. Sakamoto, T.-j. Min, S.-a. Roh, K. Yoshikawa, Fuel Process. Technol. 91 (2010) 951.
[9] G. Elordi, M. Olazar, M. Artetxe, P. Castaño, J. Bilbao, Appl. Catal. A: Gen. 415–416 (2012) 89.
[10] H. Ago, N. Uehara, N. Yoshihara, M. Tsuji, M. Yumura, N. Tomonaga, T. Setoguchi, Carbon 44 (2006) 2912.
[11] J.C. Acomb, C.F. Wu, P.T. Williams, Appl. Catal. B-Environ. 180 (2016) 497.
[12] I. Barbarias, G. Lopez, M. Artetxe, A. Arregi, L. Santamaria, J. Bilbao, M. Olazar, J. Anal. Appl. Pyrol. 122 (2016) 502.
[13] C. Wu, P.T. Williams, Appl. Catal. B: Environ. 87 (2009) 152.
[14] C. Wu, P.T. Williams, Appl. Catal. B: Environ. 96 (2010) 198.
[15] C. Wu, P.T. Williams, Int. J. Hydrogen Energy 34 (2009) 6242.
[16] S. Kumagai, J. Alvarez, P.H. Blanco, C. Wu, T. Yoshioka, M. Olazar, P.T. Williams, J. Anal. Appl. Pyrol. 113 (2015) 15.
[17] M.A. Nahil, C. Wu, P.T. Williams, Fuel Process. Technol. 130 (2015) 46.
[18] C. Wu, P.T. Williams, Appl. Catal. B: Environ. 90 (2009) 147.
[19] R.V. Salvatierra, G. Zitzer, S.A. Savu, A.P. Alves, A.J.G. Zarbin, T. Chassé, M.B. Casu, M.L.M. Rocco, Synthetic Met. 203 (2015) 16.
[20] A. Aqel, K.M.M.A. El-Nour, R.A.A. Ammar, A. Al-Warthan, Arabian J. Chem. 5 (2012) 1.
[21] K.A. Shah, B.A. Tali, Mater. Sci. Semicon. Proc. 41 (2016) 67.
[22] Q. Zhao, T. Jiang, C. Li, H. Yin, J. Ind. Eng. Chem. 17 (2011) 218.
[23] F. Danafar, A. Fakhru'l-Razi, M.A. Mohd Salleh, D.R. Awang Biak, Chem. Eng. Res. Des. 89 (2011) 214.
[24] A. Gorbunov, O. Jost, W. Pompe, A. Graff, Appl. Surf. Sci. 197–198 (2002) 563.
[25] R.T.K. Baker, J. Catal. 37 (1975) 101.
[26] M.S. Kim, N.M. Rodriguez, R.T.K. Baker, J. Catal. 131 (1991) 60.
[27] E.F. Kukovitskii, L.A. Chernozatonskii, S.G. L'Vov, N.N. Mel'nik, Chem. Phys. Lett. 266 (1997) 323.
[28] J. Liu, Z. Jiang, H. Yu, T. Tang, Polym. Degrad. Stabil. 96 (2011) 1711.
[29] N. Mishra, G. Das, A. Ansaldo, A. Genovese, M. Malerba, M. Povia, D. Ricci, E. Di Fabrizio, E. Di Zitti, M. Sharon, M. Sharon, J. Anal. Appl. Pyrol. 94 (2012) 91.
[30] S. Takenaka, M. Serizawa, K. Otsuka, J. Catal. 222 (2004) 520.
[31] J.C. Acomb, C. Wu, P.T. Williams, Appl. Catal. B: Environ. 147 (2014) 571.
[32] J.M. Saad, M.A. Nahil, P.T. Williams, J. Anal. Appl. Pyrol. 113 (2015) 35.
[33] A. Erkiaga, G. Lopez, I. Barbarias, M. Artetxe, M. Amutio, J. Bilbao, M. Olazar, J. Anal. Appl. Pyrol. 116 (2015) 34.
[34] R.R. Soares, D.F. Martins, D.E.S. Pereira, M.B. Almeida, Y.L. Lam, J. Mol. Catal. A: Chem. 422 (2016) 142.
[35] C. Wu, L. Dong, J. Onwudili, P.T. Williams, J. Huang, ACS Sustain. Chem. Eng. 1 (2013) 1083.
[36] L. Karam, S. Casale, H. El Zakhem, N. El Hassan, J. CO_2 Util. 17 (2017) 119.
[37] F. Auprêtre, C. Descorme, D. Duprez, Catal. Commun. 3 (2002) 263.
[38] J.C. Acomb, C. Wu, P.T. Williams, Appl. Catal. B: Environ. 180 (2016) 497.
[39] C.J. Lee, J. Park, J.A. Yu, Chem. Phys. Lett. 360 (2002) 250.
[40] F. Danafar, A. Fakhru'l-Razi, M.A.M. Salleh, D.R.A. Biak, Chem. Eng. J. 155 (2009) 37.
[41] M. Anna, G.N. Albert, I.K. Esko, J. Phys.: Condens. Matter 15 (2003) S3011.
[42] W.-W. Liu, A. Aziz, S.-P. Chai, A.R. Mohamed, U. Hashim, J. Nanomater. 2013 (2013) 8.
[43] W.Y. Liu, J.L. Jiang, Neural Comput. Appl. (2013) 1.
[44] W.X. Liu, T.J. Chin, G. Carneiro, D. Suter, Point correspondence validation under unknown radial distortion, Digital Image Computing: Techniques and Applications (DICTA), 2013 International Conference, 26–28 Nov, 2013, 2013, p. 1.
[45] A.L.M. da Silva, J.P. den Breejen, L.V. Mattos, J.H. Bitter, K.P. de Jong, F.B. Noronha, J. Catal. 318 (2014) 67.
[46] D.L. Trimm, Catal. Today 37 (1997) 233.
[47] D. Chen, K.O. Christensen, E. Ochoa-Fernández, Z. Yu, B. Tøtdal, N. Latorre, A. Monzón, A. Holmen, J. Catal. 229 (2005) 82.
[48] C.L. Cheung, A. Kurtz, H. Park, C.M. Lieber, J. Phys. Chem. B 106 (2002) 2429.
[49] F. Ding, A. Rosen, K. Bolton, J. Chem. Phys. 121 (2004) 2775.